JOURNAL OF NATURAL PRODUCTS

pubs.acs.org/jnp

Article

Enigmazole C: A Cytotoxic Macrocyclic Lactone and Its Ring-Opened Derivatives from a New Species of *Homophymia* Sponge

Guillermo Tarazona, Rogelio Fernández, Marta Pérez, Ramón E. Millán, Carlos Jiménez,* Jaime Rodríguez,* and Carmen Cuevas

Cite This: *J. Nat. Prod.* 2022, 85, 1059−1066

Read Online

ACCESS | Metrics & More | Article Recommendations | Supporting Information

ABSTRACT: A new macrolide, enigmazole C (**1**), and two additional analogues, enigmazoles E (**2**) and D (**3**), were obtained from a new species of the *Homophymia* genus as part of an ongoing discovery program at PharmaMar to study cytotoxic substances from marine sources. The structures were fully characterized by cumulative analyses of NMR, IR, and MS spectra, along with density functional theory computational calculations. All three of the new compounds feature an unusual 2,3-dihydro-4*H*-pyran-4-one moiety, but only enigmazoles C (**1**) and D (**3**) showed cytotoxic activity in the micromolar range against A-549 (lung), HT-29 (colon), MDA-MB-231 (breast), and PSN-1 (pancreas) tumor cells.

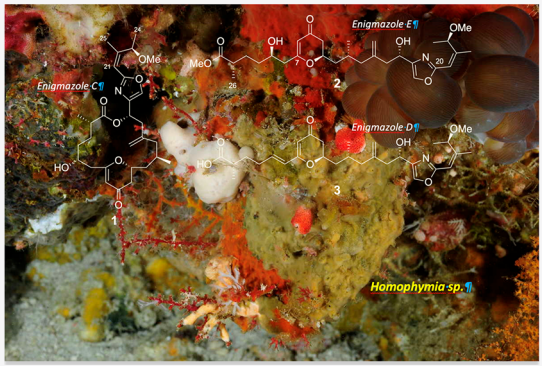

Marine sponges represent a prolific source of structurally unique macrolides possessing promising biological activities, including cytotoxic, anticancer, and neuroprotective properties, thus suggesting their potential value for the development of leads in drug discovery.[1] Particularly, sponges from the Neopeltidae family have not been extensively chemically investigated, with relatively few structures being described in the literature from each of the three genera *Homophymia*, *Callipelta*, and *Daedalopelta*. By way of illustration, the high molecular weight peptides homophymines A−E/A1−E1,[2,3] homophymamide A,[4] pipecolidepsins A−C,[5−7] and callipeltins A and B,[8−10] have all been reported to have significant cytotoxic and anti-HIV activities. Others metabolites isolated from Neopeltidae sponges that were assigned in 2013 to the suborder Astrophorina[11,12] are the bioactive tetramic acid glycoside aurantoside C[13] and the macrocycles callipeltosides A−C.[14,15] Furthermore, only two structures belonging to the *Daedalopelta* genus have been described, the cytotoxic cyclodepsipeptide daedophamide[16] and the 14-membered macrolide neopeltolide,[17] which has been extensively studied and synthesized because it is a potent cytochrome bc1 complex inhibitor, as well as a cytotoxic compound with activity against A-549 human lung adenocarcinoma, NCI/ADR-Res ovarian sarcoma, and P388 murine leukemia cell lines.[18−21]

During continuing efforts at PharmaMar to discover new cytotoxic compounds from marine natural sources, we have evaluated a new sponge species of the *Homophymia* genus (Vacelet & Vasseur, 1971) collected off the coast of Gorontalo, Indonesia. In this paper, we describe the isolation of a new macrocyclic compound as well as two open-chain analogues, all isolated from a specimen of this sponge collected in Indonesia. Despite the fact that the new macrocycle shows structural similarities to neopeltolide, a clear resemblance to the macrolide enigmazole A isolated by Oku et al. in 2010 from the marine sponge *Cynachyrella enigmatica*,[22] has led us to designate the three new compounds as enigmazoles C (**1**), E (**2**), and D (**3**). The configurations of these enigmazoles have been solved using a combination of microscale chemical conversions and the use of an elegant *J*-based configurational analysis based on capillary NMR measurements.[23]

A methanolic extract of the *Homophymia* sponge specimen showed cytotoxic activity against A-549 (lung), HT-29 (colon), MDA-MB-231 (breast), and PSN-1 (pancreas) tumor cells and was hence selected for a more detailed bioassay-guided chemical investigation.

Careful fractionation of the MeOH extract led to isolation of the new macrolide enigmazole C (**1**, 2.9 mg), and two open-chain derivatives, enigmazole D (**3**, 0.4 mg) and the methanolic adduct enigmazole E (**2**, 1.4 mg), which were purified by semipreparative HPLC.

Enigmazole C (**1**) was isolated as a colorless amorphous solid and showed a $[M + H]^+$ ion at m/z 516.2964 (calcd for

Received: December 13, 2021
Published: March 2, 2022

https://doi.org/10.1021/acs.jnatprod.1c01179
J. Nat. Prod. 2022, 85, 1059−1066

Chart 1. Structures of Enigmazoles C (1), E (2), and D (3) and Known Enigmazole A (4)

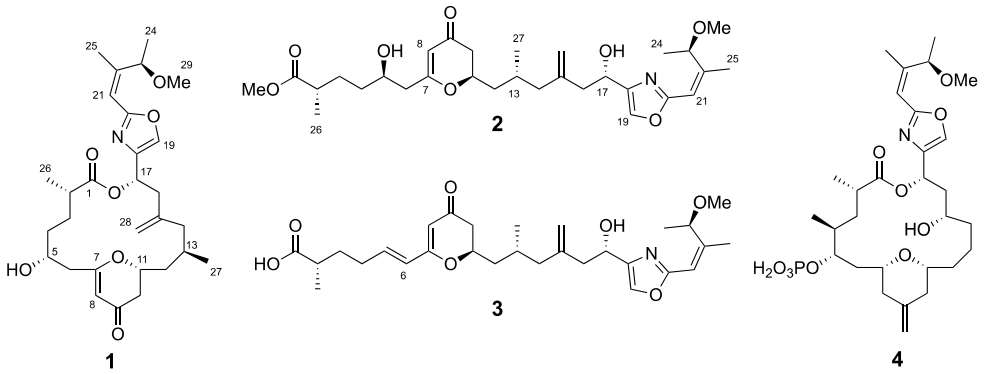

$C_{29}H_{42}NO_7$ *m/z* 516.2956) in its (+)-HR-ESITOF-MS spectrum. The presence of the sodium adduct at *m/z* 538.2785 (calcd for $C_{29}H_{41}NO_7Na$ *m/z* 538.2775) confirmed the molecular formula and 10 degrees of unsaturation required for this compound.

NMR experiments of **1** were carried out in CD_3CN because a chemical transformation was observed using CD_3OD. ^1H, ^{13}C, and edited-HSQC NMR analysis of **1** revealed the presence of 29 carbons assigned to seven sp^2 nonprotonated carbons (δ_C 193.6, 175.6, 175.5, 161.2, 152.7, 143.9, and 141.7), three sp^2 methine carbons (δ_H/δ_C 7.63/135.9, 6.20/113.6, and 5.30/106.8), a disubstituted exomethylene moiety (δ_H/δ_C 4.91; 4.86/113.9), six sp^3 methine carbons (δ_H/δ_C 5.92/66.7, 5.20/75.5, 4.48/77.8, 3.74/69.5, 2.49/39.9, and 2.20/25.8), seven sp^3 methylene carbons (δ_H/δ_C 2.72; 2.62/42.2, 2.49; 2.27/44.6, 2.49; 1.59/40.2, 2.41; 2.23/42.2, 1.81; 1.46/42.9, 1.69; 1.63/30.8 and 1.43; 1.31/34.5), and five methyl groups (δ_H/δ_C 3.15/56.6 (OMe), 1.86/17.7, 1.23/19.5, 1.10/17.6, and 0.95/21.2).

Two-dimensional COSY, 2D-TOCSY, and selective 1D-TOCSY experiments of **1** allowed us to identify five different spin systems, fragments **A** (C23−C24), **B** (C21−C25), **C** (C16−C19), **D** (C2−C6, C26), and **E** (C10−14, C27) (Figure 1). Special attention was paid to fragments **D** and **E**

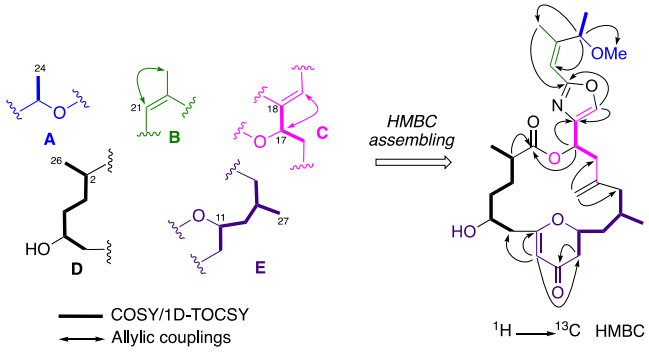

Figure 1. Spin systems deduced by COSY and 1D-TOCSY experiments and HMBC assembling in **1**.

due to the presence of four stereogenic centers. Thus, the spin system **D** was identified by selective 1D-TOCSY from selective irradiation of proton H-5 at δ_H 3.74, which gave responses to the methylene protons at δ_H 1.69/1.63 (H_2-3), δ_H 1.43/1.31 (H_2-4), and δ_H 2.49/2.27 (H_2-6), as well as the methine at δ_H 2.49 (H-2), the methyl group at δ_H 1.10 (H_3-26), and a broad signal at δ_H 3.00 assigned to a hydroxy proton (Figure 2b).

In the same way, fragment **E** was deduced by selective 1D-TOCSY irradiation of H-11 at δ_H 4.48, which showed coupling responses to three methylenes at δ_H 2.41/2.23 (H_2-10), δ_H 1.81/1.46 (H_2-12), and δ_H 2.49/1.59 (H_2-14), the methine H-13 (δ_H 2.20), and the methyl group δ_H 0.95 (H_3-27) (Figure 2c).

The interconnection between the determined fragments **A**−**E** was achieved by using an HMBC experiment as follows:

(a) The methine at δ_H 5.20 (H-23) showed long-range correlation with three methyl groups at δ_C 19.5 (C-24), δ_C 17.7 (C-25), and δ_C 56.6 (C-29), along with the sp^2 methine carbon at δ_C 113.6 (C-21), implying the position of the methoxy group on C-23 and the connection between fragments **A** and **B**.

(b) The HMBC cross-peak observed from H-21 (δ_H 6.20) to C-22 (δ_C 152.7) placed a nonprotonated carbon in the double bond. On the other hand, the singlet at δ_H 7.63 (δ_C 135.9) presented a typical chemical shift and $^1J_{CH}$ of 210 Hz of a 2,4-disubstituted oxazole ring, which was completed by inspection of the HMBC correlations observed between the oxazolic proton H-19 to carbons C-18 (δ_C 141.7) and C-20 (δ_C 161.2). The connection between fragments **B** and **C** was undoubtedly determined by the HMBC cross-peak from H-25 (δ_H 1.86) to C-20 (δ_C 161.2).

(c) Fragments **D** and **E** were connected through a six-membered ring by the cross-peaks observed from δ_H 5.30 (H-8) to δ_C 44.6 (C-6), δ_C 42.2 (C-10), and to a nonprotonated oxygenated sp^2 carbon at δ_C 175.5 (C-7). A dihydropyranone ring was deduced by the observation of the HMBC correlations from both diastereotopic protons at H-10_a (δ_H 2.41) and H10_b (δ_H 2.23) to an α,β-unsaturated carbonyl signal at δ_C 193.6.

(d) Fragments **C** and **E** were linked by a disubstituted exomethylene group as the HMBC correlations observed of H-28 (δ_H 4.86) with C-14 (δ_C 40.2) and C-16 (δ_C 42.2).

(e) A cross-peak from H-17 (δ_H 5.92) to C-1 (δ_C 175.6) allowed us to connect fragments **C** and **D**, therefore assembling the cyclic macrolactone planar structure for **1** as is drawn in Figure 1.

At this point, the resemblance of **1** to the known compound enigmazole A (**4**) was clear, as some structural features are common in both compounds: a disubstituted oxazole ring, a pyran ring, the presence of an exomethylene double bond, and a similar macrolactone size. Once the planar structure of **1** was established, the relative and absolute configuration were

https://doi.org/10.1021/acs.jnatprod.1c01179
J. Nat. Prod. 2022, 85, 1059−1066

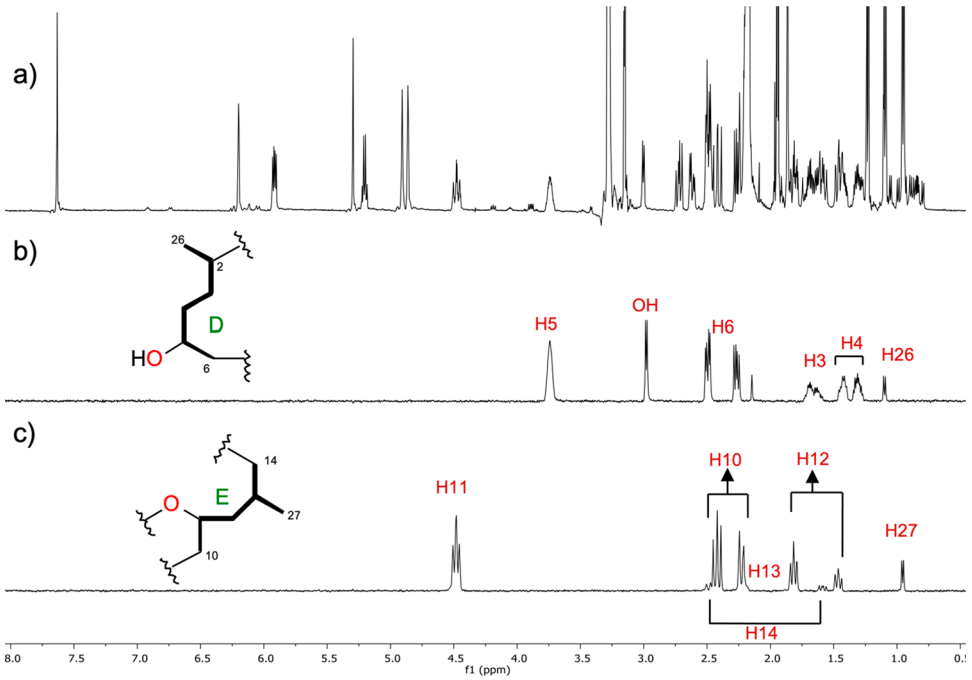

Figure 2. (a) NMR spectrum of enigmazole C (**1**) in CD_3CN at 500 MHz. Selective 1D-TOCSY irradiation experiments at (b) δ_H 3.74 (H-5) and (c) δ_H 4.48 (H-11) to identify fragments **D** and **E**.

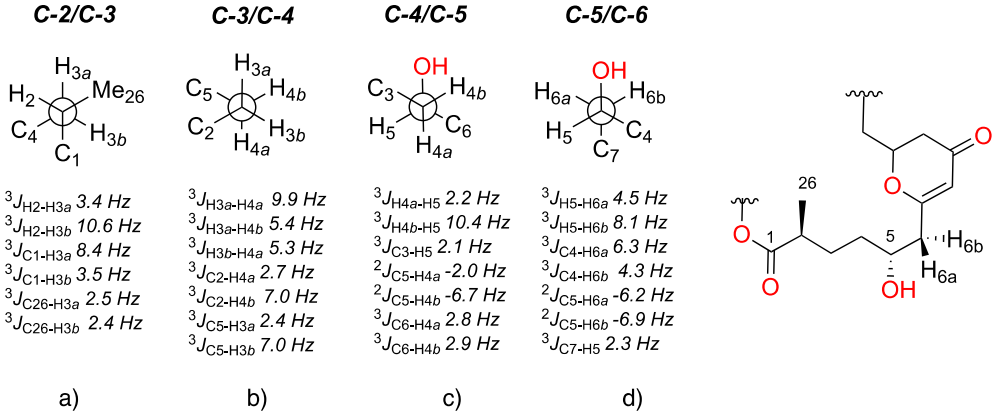

Figure 3. C-2 to C-6 fragment deduced by *J*-based configurational analysis.

determined by ROESY experiments, derivatization reactions, and computational calculations.

First, the *Z* configuration of the C-21/C-22 double bond was deduced from the ROESY correlation between H_3-25 (δ_H 1.86) and H-21 (δ_H 6.20).

To deduce the relative configuration of the entire spin system **D**, we were nicely able to relate the two stereogenic centers at C-2 and C-5 located three carbon−carbon bonds away through a *J*-based configurational analysis (JBCA).[24] To make this possible, we had to change the NMR solvent to acetone-d_6, because it gave us a ^{1}H NMR spectrum where the two diastereotopic pairs at C-3 (H-3a and H-3b) and C-4 (H-4a and H-4b) are well separated and fully resolved.

Not many approaches of this kind have been applied to a natural compound with two sp^3 methylenes surrounded by two stereogenic centers, even though this approximation is a very good tool when the diastereotopic protons can be unequivocally assigned with their corresponding chemical shifts and their sets of proton−proton and carbon−proton coupling constants. Therefore, ^{13}C−^{1}H-HSQC-TOCSY-HECADE and *J*-HMBC experiments were needed to measure key small coupling constants for $^3J_{C26-H3a}$ and $^3J_{C26-H3b}$ to place H_3-26 in a *gauche* disposition to both H-3 diastereotopic protons at the C-2/C-3 single bond (Figure 3a). These two experiments along with selective ^{1}H NMR irradiation spectra were satisfactory to deduce relationships from diastereotopic protons H-3a/H-3b and H-4a/H-4b to C-2 and C-5 as is drawn Figure 3b) for the C-3/C-4 bond. The hydroxylated carbon at C-5 helped us to deduce the relative dispositions for H-4a and H-4b to the OH group with regard to the C-4/C-5 bond (Figure 3c), as well as H-6a and H-6b to the mentioned OH relative to the C-5/C-6 bond (Figure 3d).

The absolute configuration at position C-5 was elucidated by the application of the modified Mosher's method (MMM).[25,26] The derivatization of the secondary alcohol with *R*- and *S*-MTPA-Cl was completed directly in pyridine-d_5 in an NMR tube to give compounds **1**-*S* and **1**-*R*, respectively. Comparison of the $\Delta\delta$ values ($\delta_S - \delta_R$) obtained from the MTPA esters (Figure 4) indicated that the absolute configuration of C-5 was *R*, which implies a C-2*S* configuration.

https://doi.org/10.1021/acs.jnatprod.1c01179
J. Nat. Prod. 2022, 85, 1059−1066

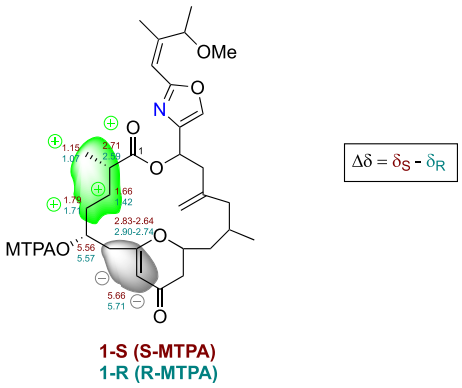

Figure 4. Mosher's derivatives of enigmazole C (**1**).

During the process of purification of enigmazole C, the use of MeOH in the HPLC separation procedure induced a macrolactone ring-opening that produces the methyl ester adduct **2**, which we have named as enigmazole E.

The (+)-HR-ESIMS-TOF data of **2** at *m*/*z* 548.3249 $[M + H]^+$ (calcd for $C_{30}H_{46}NO_8$, *m*/*z* 548.3218) and the ^{1}H NMR of **2** revealed the opening of the macrolactone ring.

Thus, the ^{1}H NMR spectrum of **2** displays a singlet signal at δ_H 3.61 (s, 3H) that was assigned to a methoxy group, which shows an HMBC correlation to an carbonyl carbon at δ_C 176.6 assigned to the new carbonyl ester at C-1. Moreover, the proton chemical shift at δ_H 5.92, assigned to H-17 in **1**, was clearly shifted to δ_H 4.72 in **2** as expected due to the lack of the lactone moiety. The presence of a hydroxy group at C-17 in **2** due to the macrolactone ring opening of **1** could be used to determine the absolute configuration at this position by the application of the MMM using the α-methoxy-α-trifluoromethylphenylacetic (MTPA) esters.

In this case, the comparison between the proton chemical shifts of both MTPA esters at C-17 (δ_2-*S* − δ_2-*R*) established the absolute configuration of C-17 as *S* (see Figure 5). In addition, the esterification of **2** with MTPA-Cl generated also the MTPA esters at C-5; the comparison of proton chemical shift values confirmed again the configuration of this stereogenic center as *R*.

To establish the configuration between C-11 and C-13 at **1**, and therefore of **2**, homonuclear coupling constants of H-11/H-12b, H-11/H-12a, H-12b/H-13, and H-12a/H-13 were extracted from selective 1D-TOCSY experiments (Figure 2c). The multiplicity observed for H-11 as a dddd with two large and two small couplings ($^3J_{H11-H10a}$ 14.1 Hz, $^3J_{H11-H10b}$ 2.7 Hz, $^3J_{H11-H12b}$ 11.0 Hz, and $^3J_{H11-H12a}$ 2.6 Hz), the heteronuclear coupling constants ($^3J_{C10-H12a}$ 1.7 Hz, $^3J_{C10-H12b}$ 1.7, $^2J_{C11-H12a}$ −5.6 Hz $^2J_{C11-H12b}$ 0 Hz), and the ROESY correlation observed between H-12b and H-10 allowed us to deduce the presence of the rotamer represented for C-11/C-12 bonds in Figure 6a.

In the same way, a large proton−proton coupling constant of 11.0 Hz between H-13 and H-12a fixed these protons in an *antiperiplanar* disposition, making necessary the use of ROESY correlations between the pairs H-12a/H-27 and H-11/H-14 and the long-range ^{13}C−^{1}H coupling constants $^3J_{C11-H13}$ 0.5 Hz, $^3J_{C27-H12a}$ 3.0 Hz, and $^2J_{C27-H12a}$ 3.0 Hz to determine the presence of the rotamer drawn in Figure 6b. Once H-12a and H-12b are interrelated to conformers **6a** and **6b**, we were able to determine the relative configuration of the two stereogenic centers C-11 and C-13 as *R** and *R**.

While the absolute configurations of C-2, C-5, and C-17 are already known as *S*, *R*, and *S*, respectively, the relative configurations of C-11 and C-13 as *R** and *R** along with the possible configuration at C-23 of either *R* or *S* give us four possible enigmazole C diastereomers (**1a**−**d**) that can be discriminated by an NMR−density functional theory (DFT) approximation. Initially we submitted all diastereoisomers to a conformational search with the Macromodel program using the protocol of Daranas, Sarotti, et al.[27] Thus, 58 conformers for **1a**-(2*S*,5*R*,11*R*,13*R*,17*S*,23*R*), 64 for **1b**-(2*S*,5*R*,11*S*,13*S*,17*S*,23*S*), 60 for **1c**-(2*S*,5*R*,11*S*,13*S*,17*S*,23*R*), and 62 for **1d**-(2*S*,5*R*,11*R*,13*R*,17*S*,23*S*) were found within a 5.0 kcal/mol window, which were further classified by energy and frequencies using the B3LYP/6-31G(d) functional. Once the duplicates and conformers with imaginary frequencies were removed, a combination of MPW1PW91/6-31G(d,p) and the polarizable continuum model was used for proton and carbon chemical shift calculations using MeCN as solvent. The sets of ^{1}H and ^{13}C chemical shifts were compared by the statistical

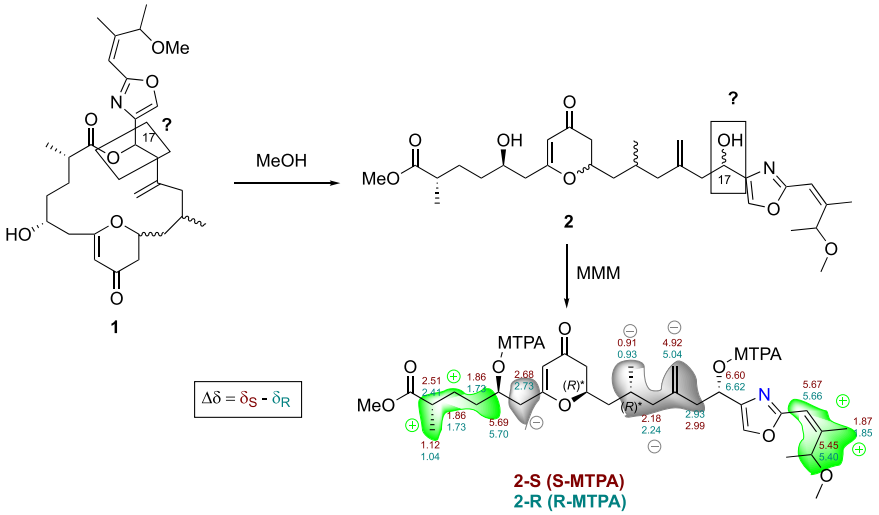

Figure 5. Modified Mosher methodology (MMM) applied to enigmazole E (**2**) to deduce the absolute configuration at C-17 and confirming the absolute configuration at C-5.

https://doi.org/10.1021/acs.jnatprod.1c01179
J. Nat. Prod. 2022, 85, 1059−1066

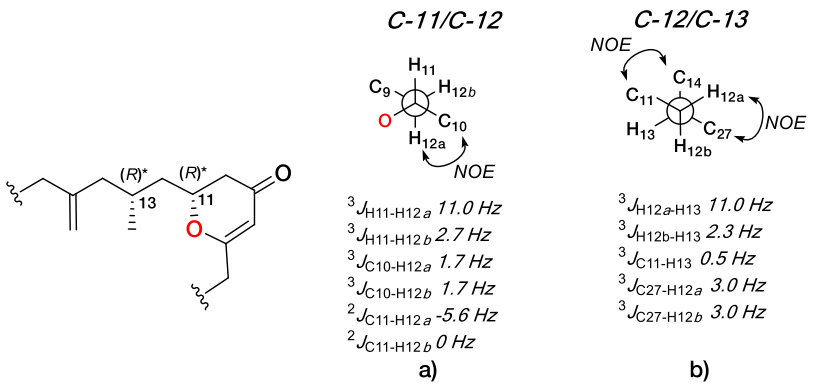

Figure 6. Rotamers along C-11/C-12 (a) and C-12/C-13 (b) bonds in enigmazole C (**1**).

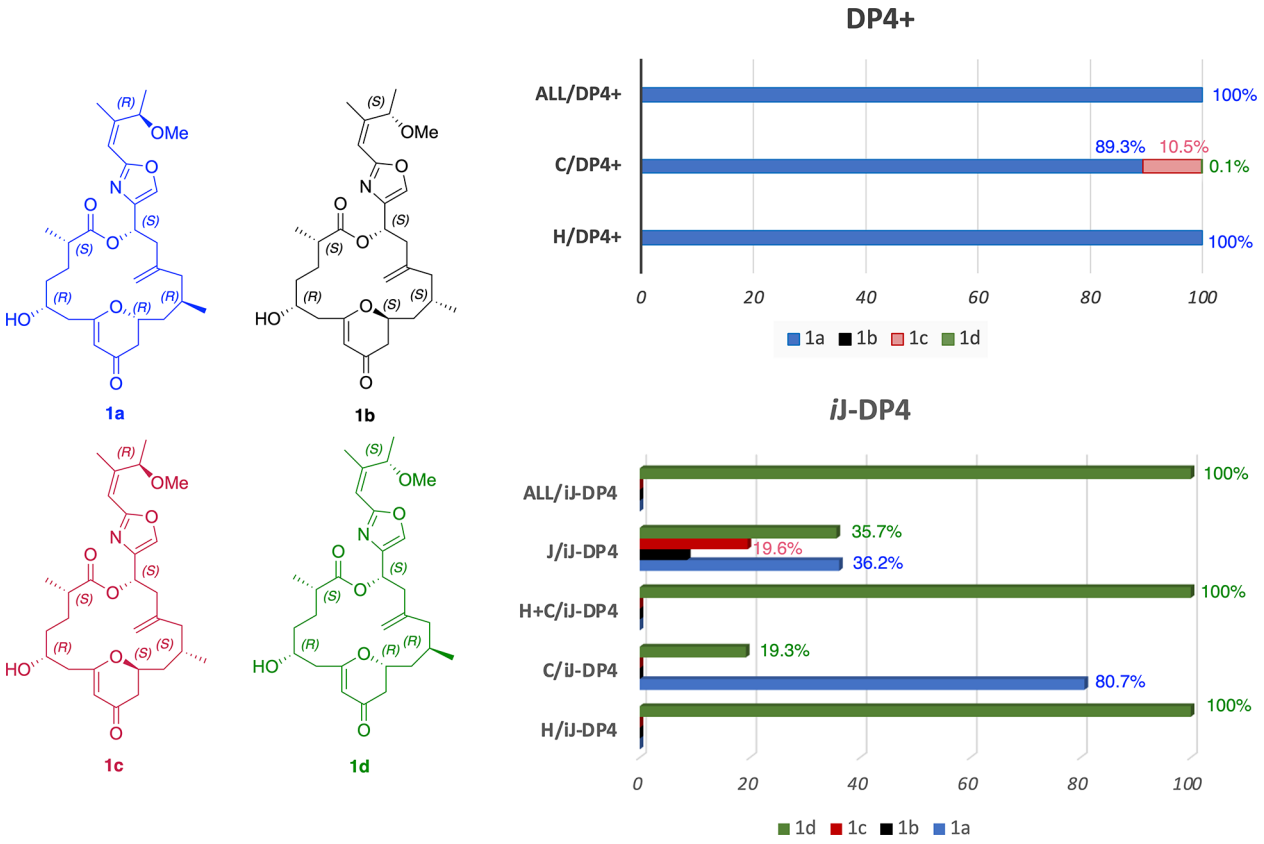

Figure 7. DP4+ and i*J*-DP4 statistical correlations of diastereoisomers **1a**-(2*S*,5*R*,11*R*,13*R*,17*S*,23*R*), **1b**-(2*S*,5*R*,11*S*,13*S*,17*S*,23*S*), **1c**-(2*S*,5*R*,11*S*,13*S*,17*S*,23*R*), and **1d**-(2*S*,5*R*,11*R*,13*R*,17*S*,23*S*) of enigmazole C.

DP4+ parameter developed by Sarotti and co-workers.[27,28] A 100% probability DP4+ value for all chemical shifts was in agreement with diastereoisomer **1a**-(2*S*,5*R*,11*R*,13*R*,17*S*,23*R*) (Figure 7).

However, when the i*J*-DP4 was computed using the suggested combination of the MMFF-5 kcal/mol conformational search and B3LYP/6-31G(d) for chemical shifts and coupling constants (just the contact Fermi contribution), no clear discrimination between isomers **1a**-(2*S*,5*R*,11*R*,13*R*,17*S*,23*R*) and **1d**-(2*S*,5*R*,11*R*,13*R*,17*S*,23*S*) was achieved when six $^3J_{HH}$ constraints were introduced.[27] Clearly both DP4+ and i*J*-DP4 were able to discriminate 11*R*,13*R* diastereoisomers **1a** and **1d** from both 11*S*,13*S*-**1b** and 11*S*,13*S*-**1c**. At this point just C-23 remains to be assigned, and since the fragment C-18/C-25 showed similar NMR values (see chemical shifts in CD_3OD in the Supporting Information) to that for enigmazole A (**4**),[22] we propose the final structure for enigmazole C (**1**) as 2*S*,5*R*,11*R*,13*R*,17*S*,23*R* (diastereoisomer **1a**). In comparison with enigmazole A, **1** presents the same configurations of the stereogenic centers at the C-2, C-5, C-11, C-13, C-17, and C-23 positions.

Along with **1**, an analogue of **3**, enigmazole D, was also found during the process of isolation and purification. Its HR-ESITOF-MS data showed the $[M + H]^+$ adduct at *m*/*z* 516.2932, which was in perfect agreement for a molecular formula of $C_{29}H_{42}NO_7$. Although the formula of **3** matches that found for enigmazole C, its HPLC retention time and ^1H NMR spectrum were different. Three new ^1H NMR signals corresponding to two vinylic protons (δ_H 6.58 and 6.00) and one oxygenated methine at δ_H 4.74, in addition to the absence

https://doi.org/10.1021/acs.jnatprod.1c01179
J. Nat. Prod. 2022, 85, 1059−1066

of the signals for H-17 (δ_H 5.92), H-5 (δ_H 3.74), and the OH group at δ_H 3.00 in **1**, lead us to suspect the opening of the macrolactone ring accompanied by an elimination of H_2O. COSY correlations of the sp^2 methine group at δ_H 6.58 with δ_H 6.00 and 2.21 and two extra signals observed from sp^2 methines, with the loss of the hydroxy group, clearly suggested the formation of a new double bond in **3**. The movement of the signal at δ_H 5.92 (H-17) found in **1** to a lower value of δ_H 4.74 in **3** along with the expected chemical shift of the new methine proton is in agreement with the opening of the lactone ring. With all these data on hand, we were able to assign the structure of enigmazole E to **3**, a metabolite resulted from the opening of enigmazole C and a further dehydration at position C-5. It is important to notice that this new double bond has an *E* configuration, based on the 15.6 Hz coupling constant found between H-5 and H-6.

Compounds **2** and **3** can be considered derivatives of enigmazole C, and therefore we assumed the absolute configurations at positions C-2, C-5 (just for compound **2**), C-11, C-13, C-17, and C-23 were the same as for **1**; thus (2*S*,5*R*,11*R*,13*R*,17*S*,23*R*) for enigmazole E (**2**) and (2*S*,11*R*,13*R*,17*S*,23*R*) for enigmazole D (**3**) were determined.

All of the new compounds were tested in a panel of four human cancer cell lines: A-549 (lung), HT-29 (colon), MDA-MB-231 (breast), and PSN-1 (pancreas). Enigmazole C (**1**) showed activity on the order of micromolar range with a GI_{50} of 9.9 μM against the A-549 cell line (Table 2). Although enigmazole D (**3**) is the open form with an additional double bond of compound **1**, cytotoxicity was observed in all cell lines (Table 3), while the methyl ester **2** of the open form of **1** renders the compound totally devoid of cytotoxicity.

In summary, the investigation of the *Homophymia* sp. sponge led to the isolation of one new macrolide lactone, enigmazole C (**1**), along with two open form congeners, enigmazoles E (enigmazole C seco acid methyl ester) (**2**) and enigmazole D (**3**). Spectroscopic data, chemical derivatization, and NMR-DFT methods were necessary to deduce the configurations of the six stereogenic centers present in their carbon skeletons. Notably, compounds **1** and **3** exhibited cytotoxic activities against A-549 (lung), HT-29 (colon), MDA-MB-231 (breast), and PSN-1 (pancreas) cell lines.

EXPERIMENTAL SECTION

General Experimental Procedures. Optical rotations were measured on a JASCO DIP-1000 polarimeter, with a Na (589 nm) lamp and filter. UV spectra were measured on a JASCO V-650 spectrophotometer. IR spectra were measured on a FTIR Bruker Vector 22 spectrometer. ^1H, ^{13}C, and 2D NMR spectra were recorded on a Varian "Unity 500" (500 MHz for ^1H and 125 MHz for ^{13}C), Varian "Unity 400" (400 MHz for ^1H and 100 MHz for ^{13}C), and Bruker Avance 500 (500 MHz for ^1H and 125 MHz for ^{13}C) with a dual cryoprobe or a BBI probe. CD_3OD, CD_3CN, C_5D_5N, and acetone-d_6 were used as deuterated solvents. Chemical shifts are reported in δ scale relative to methanol-d_4 (δ 3.31 ppm for ^1H NMR, δ 49.0 ppm for ^{13}C NMR), acetonitrile-d_3 (δ 1.94 ppm for ^1H NMR, δ 1.32 ppm for ^{13}C NMR), acetone-d_6 (δ 2.05 ppm for ^1H NMR, δ 29.84 ppm for ^{13}C NMR), and pyridine-d_5 (δ 8.74 ppm for ^1H NMR, δ 150.35 ppm for ^{13}C NMR). HSQC-TOCSY-HECADE experiments were acquired with 32 scans and 256 increments with a mixing time of 60 ms and 4K points. J-HMBC was run with 16 scans, 200 increments, and 2 K points in F2.

LRESIMS and HRESIMS experiments were performed on the Applied Biosystems QSTAR Elite system or on an Agilent 6230 TOF LC/MS. HPLC separation was performed on an Agilent 1100 or 1200 using reversed-phase chromatographic columns.

Table 1. NMR Data of Enigmazole C (1) in CD_3CN and Acetone-d_6

	CD_3CN δ_H, m (*J* in Hz)		acetone-d_6	
pos.	δ_C, type	δ_H, m (*J* in Hz)	δ_C	δ_H, m (*J* in Hz)
1	175.6, C		174.9	
2	39.9, CH	2.49, m	39.7	2.53 ddq (10.6, 6.9, 3.4)
3	30.8, CH_2	a: 1.69, m	30.8	a: 1.79, dddd (13.8, 9.9, 5.4, 3.4)
		b: 1.63, m		b: 1.68, dddd (13.8, 10.6, 5.3, 5.3)
4	34.5, CH_2	a: 1.43, m	34.5	a: 1.51, dddd (14.4, 9.9, 5.3, 2.2)
		b: 1.31, m		b: 1.38, dddd (14.4, 10.4, 5.4, 5.3)
5	69.5, CH	3.74, ddddd (10.4, 7.6, 5.5, 5.5, 2.5)	69.6	3.83, ddddd (10.4, 8.1, 5.8, 4.5, 2.2) 2.2)
6	44.6, CH_2	a: 2.49, dd (13.2, 5.5)	44.9	a: 2.59, dd (13.1, 4.5)
		b: 2.27, dd (13.2, 7.6)		b: 2.31, dd (13.1, 8.1)
7	175.5, C		174.8	
8	106.8, CH	5.30, d (1.0)	106.8	5.28, bs (1.0)
9	193.6, C		192.4	
10	42.2, CH_2	a: 2.41, dd (16.7, 14.0)	42.3	a: 2.41, dd (16.7, 14.0)
		b: 2.23, dd (16.7, 2.6)		b: 2.26, dd (16.7, 2.7)
11	77.8, CH	4.48, ddt (14.0, 11.0, 2.6, 2.6)	77.4	4.53 ddt (14.0, 11.0, 2.7, 2.7)
12	42.9, CH_2	a: 1.81, ddd (14.2, 10.9, 2.6)	43.1	a: 1.85, ddd (14.1, 11.0, 2.7)
		b: 1.46, dd (14.2, 11.0)		b: 1.54, ddd (14.2, 11.1, 2.3)
13	25.8, CH	2.20, m	25.6	2.29, m
14	40.2, CH_2	a: 2.49, dd (15.8, 1.5)	40.0	a: 2.27, dd (16.0, 2.7)
		b: 1.59, dd (15.8, 10.7)		b: 1.61, dd (16.0, 11.0)
15	143.9, C		143.8	
16	42.2, CH_2	a: 2.72, dd (13.7, 9.6)	42.3	a: 2.75, dd (13.8, 9.7)
		b: 2.62, dd (13.7, 5.2)		b: 2.67, dd (13.8, 5.1)
17	66.7, CH	5.92, ddd (9.4, 5.2, 0.8)	66.3	6.00, dd (9.7, 4.9)
18	141.7, C		142.0	
19	135.9, CH	7.63, d (0.7)	135.6	7.77, s
20	161.2, C		161.0	
21	113.6, CH	6.20, dd (1.5, 0.8)	113.5	6.21, bs
22	152.7, C		152.4	
23	75.5, CH	5.20, dq (6.5, 0.8)	75.3	5.29, bq (6.5)
24	19.5, CH_3	1.23, d (6.5)	19.4	1.24, d (6.5)
25	17.7, CH_3	1.86, d (1.5)	17.5	1.88, d (1.6)
26	17.6, CH_3	1.10, d (6.9)	17.6	1.11, d (6.9)
27	21.2, CH_3	0.95, d (6.7)	21.2	0.98, d (6.6)
28	113.9, CH_2	a: 4.91, s	113.5	a: 4.94, s
		b: 4.86, s		b: 4.88, s
29	56.6, CH_3	3.15, s	56.5	3.17, s
OH	-	3.00, d (6.0)	-	3.90 d (5.8)

Animal Material. The sponge belongs to the genus *Homophymia* Vacelet and Vasseur, 1971. It was collected by hand using a rebreather diving system in Gorontalo, Indonesia (01° 19.836′ S/122° 45.022′ E) at depths ranging between 40 and 80 m. The animal material was identified by Dr. María Jesús Uriz (Center for Avanced Studies of Blanes). A sample of the specimen was deposited in the Center for

https://doi.org/10.1021/acs.jnatprod.1c01179
J. Nat. Prod. 2022, 85, 1059−1066

Table 2. Cytotoxic Activities for Enigmazole C (1)

cell line	GI_{50}	TGI	LC_{50}
A-549	9.9 μM	>19 μM	>19 μM
HT-29	18 μM	>19 μM	>19 μM
MDA-MB-231	>19 μM	>19 μM	>19 μM
PSN-1	87 μM	>19 μM	>19 μM

Table 3. Cytotoxic Activities for Enigmazole D (3)

cell line	GI_{50}	TGI	LC_{50}
A-549	1.4 μM	>19 μM	>19 μM
HT-29	1.0 μM	3.7 μM	>19 μM
MDA-MB-231	4.1 μM	>19 μM	>19 μM
PSN-1	1.1 μM	>19 μM	>19 μM

Advanced Studies of Blanes in Girona, Spain, with the reference code GORO-093. In addition, a voucher specimen (ORMA136284) was deposited at PharmaMar.

Description: Thickly globular sponge (3 cm high, 4 cm wide, 2 cm tick), smooth without conulous projections. Hard consistency, white color, and small single oscule in apical position. Megascleres: fine monoactines spicules broken in their preparations. Desmas pseudotetraclones with very tuberculated zygomes. Ectosomal megascleras are smooth pesudophyllotriaenes with different irregular pseudocladis tuberculated in the same specimen. Microscleres consist of a single type of microspinose amphiasters occurring in different size classes: the smaller 10−15 μm long, the larger 12−25 μm long.

Extraction and Isolation. A specimen of *Homophymia* (33 g) was triturated and exhaustively extracted with $MeOH/CH_2Cl_2$ (50:50, 3 × 500 mL). The combined extracts were concentrated to yield a mass of 2.5 g, which was subjected to VLC on Lichroprep RP-18 (Merck KGaA) with a stepped gradient from H_2O to MeOH and then CH_2Cl_2. The fraction eluting with MeOH (96 mg) was subjected to semipreparative HPLC (Ascentis C18, 5 μm, 410 × 150 mm, isocratic H_2O/MeCN (60:40) for 3 min, gradient H_2O/MeCN from 50% to 65% MeCN in 25 min, UV detection, flow 1 mL/min, t_r: 19.5 min to give compound **1** (2.9 mg), 12.0 min to give compound **2** (1.4 mg), and 13.0 min to give compound **3** (0.4 mg)).

*Enigmazole C (**1**):* amorphous, yellow oil; $[\alpha]_D$ +56 (*c* 0.03, MeOH); UV (MeOH) λ_{max} 261 nm; IR (ATR) ν_{max} 3378, 2966, 2311, 1675, 1140 cm^{-1}; ^1H NMR (500 MHz) and ^{13}C NMR (125 MHz), Table 1; (+)-HRESI-TOFMS *m/z* 516.2964 $[M + H]^+$ (calcd for $C_{29}H_{42}NO_7$, 516.2956); *m/z* 538.2785, $[M + Na]^+$ (calcd for $C_{29}H_{41}NO_7Na$).

*Enigmazole E (enigmazole C seco acid methyl ester, **2**):* yellow oil; UV (MeOH) λ_{max} 265 nm; ^1H and ^{13}C NMR, Table S1; (+)-HRESI-TOFMS *m/z* 548.3249 $[M + H]^+$ (calcd for $C_{30}H_{46}NO_8$, 548.3218).

*Enigmazole D (**3**):* yellow oil; UV (MeOH) λ_{max} 254, 277, 286 nm; ^1H and ^{13}C NMR, Table S2; (+)-HRESI-TOFMS *m/z* 516.2932 $[M + H]^+$ (calcd for $C_{29}H_{42}NO_7$, 516.2956).

Computational Calculations. Conformational searches were performed by using the corresponding module implemented in the Maestro Quantum mechanical software. The MMFF force field with acetonitrile as solvent was used, and torsional enhanced sampling with 10 000 steps was fixed using an energy window of 5 kcal/mol.

DP4+. Molecular geometry optimizations were performed for **1a**−**d** at the DFT theoretical level using the Gaussian 16W package first at the B3LYP/6-31G(d) level for energy and frequency calculations. After removing redundant conformers and those with imaginary frequencies, theoretical Boltzmann energy population-weighted ^1H and ^{13}C NMR were calculated by using the combination MPW1PW91/6-31G(d,p). Results were input in Sarotti's and Darana's Excel spreadsheet[27] to calculate the best fit.

iJ-DP4. MMFF conformers at 5 kcal/mol were filtered by six proton−proton vicinal coupling restriction: $^3J_{H11H12a}$, $^3J_{H11H12b}$, $^3J_{H5H4b}$, $^3J_{H5H4a}$, $^3J_{H2H3b}$, and $^3J_{H2H3a}$. Those conformers were chosen to calculate the population-weighted Boltzmann MMFF energy. ^1H and ^{13}C NMR and $^1H-^1H$ coupling constants (just the Fermi's contact contribution) were then calculated by the combination B3LYP/6-31G(d). Results were input in Sarotti's and Darana's Excel spreadsheet[27] to calculate the best fit.

Preparation of the (*S*)-MTPA Ester of Enigmazole C (1-*S*). *R*-(−)-MTPA chloride (10 μL) was added to a solution of **1** (1.0 mg) in 0.5 mL of pyridine-d_5 in an NMR tube. The resulting mixture was allowed to stand at room temperature (rt) for 8 h to yield the (*R*)-MTPA ester of **1**, which was monitored by recording ^1H NMR spectra at 500 MHz. ^1H NMR (500 MHz, C_5D_5N) δ 5.66 (s, H-8), 5.56 (m, H-5), 2.83 (dd, *J* = 13.7, 5.1 Hz, H-6a), 2.71 (m, H2), 2.64 (dd, *J* = 13.7, 7.2 Hz, H-6b), 1.79 (m, H-4), 1.66 (m, H-3), 1.15 (d, *J* = 6.8 Hz, H-26).

Preparation of the (*R*)-MTPA Ester of Enigmazole C (1-*R*). Treatment of **1** (1.0 mg) in the same manner as before with *S*-(+)-MTPA chloride (10 μL) gave the (*R*)-MTPA ester of **1**. ^1H NMR (500 MHz, C_5D_5N) δ 5.71 (s, H-8), 5.57 (m, H-5), 2.90 (dd, *J* = 13.8, 5.0 Hz, H-6a), 2.59 (m, H-2), 2.74 (dd, *J* = 13.8, 7.0 Hz, H-6b), 1.71 (m, H-4), 1.42 (m, H-3), 1.07 (d, *J* = 6.8 Hz, H-26).

Preparation of the (*S*)-MTPA Ester of Enigmazole E (2-*S*). *R*-(−)-MTPA chloride (10 μL) was added to a solution of **2** (0.4 mg) in 0.5 mL of pyridine-d_5 in an NMR tube. The resulting mixture was allowed to stand at rt for 8 h to yield the (*S*)-MTPA ester of **2**, which was monitored by recording ^1H NMR spectra at 500 MHz. ^1H NMR (500 MHz, C_5D_5N) δ 6.60 (dd, *J* = 7.2, 7.2 Hz, H-17), 5.69 (m, H-5), 5.67 (s, H-21), 5.45 (d, *J* = 6.4 Hz, H-23), 4.92 (s, H-28), 2.93 (m, H-16), 2.68 (m, H-6), 2.51 (m, H-2), 2.18 (m, H-14), 1.87 (s, H-25), 1.86 (m, H-3), 1.86 (m, H-4), 1.12 (d, 7.0 Hz, H-26), 0.91 (d, 5.9 Hz, H-27).

Preparation of the (*R*)-MTPA Ester of Enigmazole E (2-*R*). Treatment of **2** (0.4 mg) in the same manner as before with *S*-(+)-MTPA chloride (5 μL) gave the (*R*)-MTPA ester of **2**. ^1H NMR (500 MHz, C_5D_5N) δ 6.62 (dd, *J* = 7.1, 7.1 Hz, H-17), 5.70 (m, H-5), 5.66 (s, H-21), 5.40 (d, *J* = 6.3 Hz, H-23), 5.04 (s, H-28), 2.99 (m, H-16), 2.73 (m, H-6), 2.41 (m, H-2), 2.24 (m, H-14), 1.85 (s, H-25), 1.73 (m, H-3), 1.73 (m, H-4), 1.04 (d, 7.0 Hz, H-26), 0.93 (d, 5.9 Hz, H-27).

Biological Assays. The cytotoxic activities of compounds **1**, **2**, and **3** were tested against A-549 human lung carcinoma cells, MDA-MB-231 human breast adenocarcinoma cells, HT-29 human colorectal carcinoma cells, and PSN-1 pancreatic adenocarcinoma cells. The concentration giving 50% inhibition of cell growth (GI_{50}) was calculated according to the procedure described in the literature. Cell survival was estimated using the National Cancer Institute (NCI) algorithm. Three dose−response parameters were calculated for **1**, **2**, and **3**.

■ ASSOCIATED CONTENT

Supporting Information

The Supporting Information is available free of charge at https://pubs.acs.org/doi/10.1021/acs.jnatprod.1c01179.

^1H, ^{13}C, and 2D NMR data of the new compounds and *J* configurational analysis of **1** (PDF)

■ AUTHOR INFORMATION

Corresponding Authors

Carlos Jiménez − *Departmento de Química, Facultad de Ciencias and Centro de Investigacions Científicas Avanzadas (CICA), Universidade de A Coruña, 15071 A Coruña, Spain;* orcid.org/0000-0003-2628-303X; Email: carlos.jimenez@udc.es

Jaime Rodríguez − *Departmento de Química, Facultad de Ciencias and Centro de Investigacions Científicas Avanzadas (CICA), Universidade de A Coruña, 15071 A Coruña, Spain;* orcid.org/0000-0001-5348-6970; Email: jaime.rodriguez@udc.es

https://doi.org/10.1021/acs.jnatprod.1c01179
J. Nat. Prod. 2022, 85, 1059−1066

Authors

Guillermo Tarazona − *R&D, PharmaMar, 28770 Madrid, Spain;* orcid.org/0000-0002-8724-3851

Rogelio Fernández − *R&D, PharmaMar, 28770 Madrid, Spain*

Marta Pérez − *R&D, PharmaMar, 28770 Madrid, Spain*

Ramón E. Millán − *Departmento de Química, Facultad de Ciencias and Centro de Investigacions Científicas Avanzadas (CICA), Universidade de A Coruña, 15071 A Coruña, Spain*

Carmen Cuevas − *R&D, PharmaMar, 28770 Madrid, Spain*

Complete contact information is available at: https://pubs.acs.org/10.1021/acs.jnatprod.1c01179

Notes

The authors declare no competing financial interest.

■ ACKNOWLEDGMENTS

We gratefully acknowledge the Expeditions, Collection and Cell Biology Departments of PharmaMar S.A.U. We also thank S. Bueno and Dra. M. J. Uriz (CEAB-Centro de Estudios Avanzados de Blanes, Spain) for determining the sponge taxonomy and S. Munt for revision of the manuscript. PharmaMar also acknowledges the Udayana University of Bali, Indonesia. J.R. and C.J. acknowledge Xunta de Galicia and CESGA for the computational resources.

■ REFERENCES

(1) Radjasa, O. K.; Vaske, Y. M.; Navarro, G.; Vervoort, H. C.; Tenney, K.; Linington, R. G.; Crews, P. Highlights of Marine Invertebrate-Derived Biosynthetic Products: Their Biomedical Potential and Possible Production by Microbial Associants. *Bioorg. Med. Chem.* 2011, *19*, pp 6658−6674 DOI: 10.1016/j.bmc.2011.07.017.

(2) Zampella, A.; Sepe, V.; Luciano, P.; Bellotta, F.; Chiara Monti, M.; Valeria D'Auria, M.; Jepsen, T.; Petek, S.; Adeline, M.-T.; Laprévôte, O.; Aubertin, A.-M.; Debitus, C.; Poupat, C.; Ahond, A. *J. Org. Chem.* **2008**, *73* (14), 5319−5327.

(3) Zampella, A.; Sepe, V.; Bellotta, F.; Luciano, P.; D'Auria, M. V.; Cresteil, T.; Debitus, C.; Petek, S.; Poupat, C.; Ahond, A. *Org. Biomol. Chem.* **2009**, *7* (19), 4037−4044.

(4) Kanki, D.; Nakamukai, S.; Ogura, Y.; Takikawa, H.; Ise, Y.; Morii, Y.; Yamawaki, N.; Takatani, T.; Arakawa, O.; Okada, S.; Matsunaga, S. *J. Nat. Prod.* **2021**, *84* (6), 1848−1853.

(5) Coello, L.; Reyes, F.; Martín, M. J.; Cuevas, C.; Fernández, R. *J. Nat. Prod.* **2014**, *77* (2), 298−303.

(6) Albericio, F.; García-Ramos, Y.; Martín-López, M. J.; Pelay Gimeno, M.; Tulla-Puche, J. Synthetic Process for the Manufacture of Pipecolidepsin Compounds. WO2014108526A1, 2014.

(7) Pelay-Gimeno, M.; García-Ramos, Y.; Jesús Martin, M.; Spengler, J.; Molina-Guijarro, J. M.; Munt, S.; Francesch, A. M.; Cuevas, C.; Tulla-Puche, J.; Albericio, F. The First Total Synthesis of the Cyclodepsipeptide Pipecolidepsin A. *Nat. Commun.* **2013**, *4*, DOI: 10.1038/ncomms335 article number: 2352.

(8) Bassarello, C.; Zampella, A.; Monti, M. C.; Gomez-Paloma, L.; D'Auria, M. V.; Riccio, R.; Bifulco, G. *Eur. J. Org. Chem.* **2006**, *2006*, 604−609.

(9) Kikuchi, M.; Konno, H. *Biosci., Biotechnol., and Biochem.* **2016**, *80* (6), 1066−1069.

(10) Krishnamoorthy, R.; Vazquez-Serrano, L. D.; Turk, J. A.; Kowalski, J. A.; Benson, A. G.; Breaux, N. T.; Lipton, M. A. *J. Am. Chem. Soc.* **2006**, *128* (48), 15392−15393.

(11) Thacker, R. W.; Hill, A. L.; Hill, M. S.; Redmond, N. E.; Collins, A. G.; Morrow, C. C.; Lori Spicer, ô; Carmack, C. A.; Zappe, M. E.; Pohlmann, D.; Hall, C.; Diaz, M. C.; Bangalore, P. V.; Francisco, S. Nearly Complete 28S RRNA Gene Sequences Confirm New Hypotheses of Sponge Evolution At. *Integrative Comparative Biol.* **2013**, *53*, 373-387.

(12) Redmond, N. E.; Morrow, C. C.; Thacker, R. W.; Diaz, M. C.; Boury-Esnault, N.; Cárdenas, P.; Hajdu, E.; Lôbo-Hajdu, G.; Picton, B. E.; Pomponi, S. A.; Kayal, E.; Collins, A. G. *Integrative and Comparative Biol.* **2013**, *53* (3), 388−415.

(13) Wolf, D.; Schmitz, F. J.; Qiu, F.; Kelly-Borges, M. *J. Nat. Prod.* **1999**, *62* (1), 170−172.

(14) Zampella, A.; D'Auria, M. V.; Minale, L.; Debitus, C.; Roussakis, C. *J. Am. Chem. Soc.* **1996**, *118* (45), 11085−11088.

(15) Zampella, A.; Valeria D'auria, M.; Minale, L.; Debitus, C. *Tetrahedron* **1997**, *53*, 3243−3248.

(16) Urda, C.; Fernández, R.; Rodríguez, J.; Pérez, M.; Jiménez, C.; Cuevas, C. Daedophamide, a Cytotoxic Cyclodepsipeptide from a Daedalopelta Sp. Sponge Collected in Indonesia. *J. Nat. Prod.* **2017**, *80* (1), 3054.

(17) Wright, A. E.; Botelho, J. C.; Guzmán, E.; Harmody, D.; Linley, P.; McCarthy, P. J.; Pitts, T. P.; Pomponi, S. A.; Reed, J. K. *J. Nat. Prod.* **2007**, *70* (3), 412−416.

(18) Fuwa, H.; Naito, S.; Goto, T.; Sasaki, M. *Angew. Chem., Int. Ed.* **2008**, *47* (25), 4737−4739.

(19) Zhu, X. L.; Zhang, R.; Wu, Q. Y.; Song, Y. J.; Wang, Y. X.; Yang, J. F.; Yang, G. F. *J. Agric. Food Chem.* **2019**, *67* (10), 2774−2781.

(20) Li, J.; Preinfalk, A.; Maulide, N. *Angew. Chem., Int. Ed.* **2019**, *58* (18), 5887−5890.

(21) Xiong, M. Q.; Chen, T.; Wang, Y. X.; Zhu, X. L.; Yang, G. F. *Bioorg. Med. Chem. Lett.* **2020**, *30* (16), 127324−127328.

(22) Oku, N.; Takada, K.; Fuller, R. W.; Wilson, J. A.; Peach, M. L.; Pannell, L. K.; McMahon, J. B.; Gustafson, K. R. *J. Am. Chem. Soc.* **2010**, *132* (30), 10278−10285.

(23) Molinski, T. F.; Morinaka, B. I. *Tetrahedron* **2012**, *68* (46), 9307−9343.

(24) Matsumori, N.; Kaneno, D.; Murata, M.; Nakamura, H.; Tachibana, K. *J. Org. Chem.* **1999**, *64* (3), 866−876.

(25) Hoye, T. R.; Jeffrey, C. S.; Shao, F. *Nat. Protoc.* **2007**, *2* (10), 2451−2458.

(26) Seco, J. M.; Quiñoá, E.; Riguera, R. *Chem. Rev.* **2004**, *104*, 17−117.

(27) Grimblat, N.; Gavín, J. A.; Hernández Daranas, A.; Sarotti, A. M. *Org. Lett.* **2019**, *21* (11), 4003−4007.

(28) Grimblat, N.; Zanardi, M. M.; Sarotti, A. M. *J. Org. Chem.* **2015**, *80* (24), 12526−12534.